

Impaired Synapse Function during Postnatal Development in the Absence of CALEB, an EGF-like Protein Processed by Neuronal Activity

René Jüttner,¹ Margret I. Moré,¹ Debashish Das,¹ Aleksei Babich,¹ Jochen Meier,² Mechthild Henning,¹ Bettina Erdmann,¹ Eva-Christiana Müller,¹ Albrecht Otto,¹ Rosemarie Grantyn,² and Fritz G. Rathjen^{1,*}

¹Max-Delbrück-Centrum
Robert-Rössle-Strasse 10
13092 Berlin
Germany

²Humboldt-University Medical School (Charité)
10117 Berlin
Germany

Summary

In an attempt to characterize the molecular components by which electric activity influences the development of synapses, we searched for cell surface proteins modulated by calcium influx and glutamate receptor activity. Here, we report that neuronal depolarization facilitates the conversion of CALEB, which results in a truncated transmembrane form with an exposed EGF domain. To characterize the role of CALEB in synapse development, synaptic features were investigated in slices of the colliculus superior from CALEB-deficient mice. In the absence of CALEB, the number of synapses and their morphological characteristics remained unchanged. However, in CALEB-deficient mice, synapses displayed higher paired-pulse ratios, less depression during prolonged repetitive activation, a lower rate of spontaneous postsynaptic currents, and a lower release probability at early but not mature postnatal stages. Our findings indicate that CALEB provides a molecular basis for maintaining normal release probability at early developmental stages.

Introduction

Once axons have reached their target region with the help of axonal guidance receptors and environmental guidance cues during development, synaptic connections are formed that might subsequently be refined and specified by various forms of neuronal network activity (Berardi et al., 2003; Goodman and Shatz, 1993; Katz and Crowley, 2002). Although the mechanisms by which changes in the neuronal resting membrane potential and in intracellular calcium levels exert their influence over the number, distribution, and features of synapses are still a matter of speculation, it is widely accepted that the specification of neuronal connections requires neuronal activity (Burrone et al., 2002). Early in development, neuronal activity might be spontaneous, such as the patterned waves observed in the retina before eye opening that affect early postnatal de-

velopment of the visual system (Feller, 1999; McCormick, 1999). Later in development, activity might be driven by sensory experience, and synapse strengthening or elimination might be selectively facilitated by neuronal activity (Goda and Davis, 2003). However, it is also clear that the establishment of synaptic contacts per se does not require the secretion of neurotransmitters (Verhage et al., 2000).

Membrane depolarization, elevations of intracellular calcium levels, and action potential generation can induce a number of molecular changes within neurons, including posttranslational modifications of synaptic proteins and regulation of gene activity (Kauselmann et al., 1999; Nedivi, 1999; West et al., 2001). For example, activity-dependent expression of CPG15 (neurtin), a GPI-linked plasma membrane protein, affects the growth of dendritic arbors (Cantalops et al., 2000; Nedivi et al., 1998), and the activity-dependent remodeling of synapses is regulated by the serum-inducible kinase (SNK) (Pak and Sheng, 2003). The expression of neuronal activity-regulated pentraxin (Narp), a member of the pentraxin family of proteins, is upregulated by seizures, and it functions as a secreted protein to trigger the aggregation of AMPA receptors on cultured spinal neurons (O'Brien et al., 1999; O'Brien et al., 2002). Class I major histocompatibility complex (MHC I) proteins become reduced upon blockade of neural activity, and they appear to be required for a complete segregation of retinal ganglion cell axons into eye-specific layers within the lateral geniculate nucleus (Huh et al., 2000). Finally, synaptic activity and action potential generation have been shown to induce the secretion of BDNF, which in turn modulates synaptic strength and neuronal connectivity (Poo, 2001).

Nonetheless, it is generally admitted that the molecular links between neuronal activity and synaptic plasticity are not yet precisely defined (Jessell and Sanes, 2000). Therefore, we have been interested in identifying cell surface proteins on neurons that are modulated by neuronal activity. In contrast to several other screens aimed at identifying genes modulated by neuronal activity (Coriveau et al., 1998; Hong et al., 2004; Konietzko et al., 1999; Nedivi et al., 1993; Tsui et al., 1996), we concentrated on cell surface proteins and analyzed their expression at the protein level. Such proteins that are modulated by activity are considered to be candidates that are implicated in the establishment of synapses and synaptic plasticity. Here, we report that CALEB, a transmembrane protein of the EGF family, previously identified by protein-protein interaction studies (Schumacher et al., 1997), also termed neuroglycan C (Yasuda et al., 1998), undergoes a conversion when neurons are depolarized by elevated KCl or by application of GluR agonists. Calcium channel blockers and GluR antagonists prevent the truncation of CALEB. Inactivation of the CALEB gene alters the release features of synapses during a critical phase of synapse development.

*Correspondence: rathjen@mdc-berlin.de

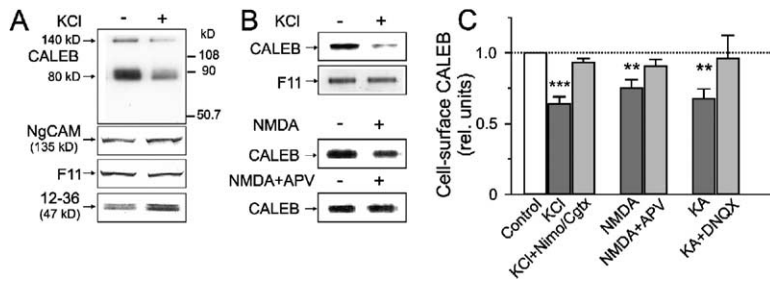


Figure 1. Activity-Dependent Downregulation of CALEB at the Cell Surface

(A) In the initial screen to identify cell surface proteins that are modulated by neural activity, chick retinal cells (prepared from E8) were cultivated for 3 days, followed by treatment with KCl (30 mM) for 12 hr. The cells were solubilized in 1% n-octylglucoside/PBS, followed by Western blotting using monoclonal antibodies. Note a decrease of CALEB, while other proteins (for example F11 and NgCAM) remained unaffected and

a protein at 47 kDa detected by mAb 12-36 increased in intensity.

(B) Retinal cells were treated with KCl (30 mM), NMDA (10 μ M), or NMDA and APV (50 μ M) for 10 min, followed by cell surface labeling using NHS-biotin. Biotinylated proteins were captured by streptavidin-agarose and analyzed in Western blots using mAb 4/1 directed to CALEB or a mAb to the F11 protein (contactin1).

(C) Quantification of biotinylated CALEB after 10 min treatment of chick retinal cell cultures with KCl (30 mM), NMDA (10 μ M), and kainate (50 μ M) in the absence or presence of the inhibitors (50 μ M APV, 10 μ M DNQX, 10 μ M nimodipine plus 1 μ M ω -conotoxin-MVIIIC). The inhibitors alone had no effect on the CALEB expression at the cell surface. $n = 6-8$, ** $p < 0.01$; *** $p < 0.001$. Error bars indicate SEM.

Results

Screens to Identify Cell Surface Proteins Modulated by Neuronal Activity

In order to identify neural cell surface proteins that are modulated by various forms of neuronal activity, we cultivated chick embryonic retinal cells in a monolayer at high density. In initial experiments, detergent extracts of chick retinal cells treated with 30 mM KCl as well as untreated control cultures were compared in Western blots using a collection of monoclonal antibodies (mAbs) to neural cell surface proteins expressed during developmental stages. A large majority of the cell surface proteins that were tested was not affected by this treatment, as shown here for the GPI-anchored contactin1 (F11) and the transmembrane protein L1 (NgCAM) (Figure 1A). However, the intensity of one cell surface protein detected by mAb 4/1, known as CALEB, appeared to be downregulated after treatment with KCl (Figure 1A), while another cell surface protein with a molecular mass of 47 kDa recognized by mAb 12-36 was upregulated in this screen. In this report, we will only consider CALEB. CALEB is expressed in several molecular mass forms and contains an EGF-like domain belonging to the EGF family of differentiation factors (Schumacher et al., 1997). The two major molecular mass forms of CALEB at 140 and 80 kDa detected by mAb 4/1 appear to be reduced upon KCl treatment (Figure 1A). However, only the 80 kDa component of CALEB, which is the dominating form in the developing chick retina, will be considered in the following. In order to analyze whether the downregulation of CALEB occurs directly at the cell surface, retinal cells were treated with elevated KCl for 10 min, followed by biotinylation with NHS-biotin, a compound unable to penetrate living cells. Cell surface proteins from treated and untreated cultures were then isolated using streptavidin-agarose and were compared by Western blotting. This analysis indicated a 35.9% ($n = 13$) decrease of the amount of plasma membrane-associated CALEB (Figures 1B and 1C). Application of GluR agonists such as NMDA (10 μ M) as well as kainate (50 μ M) also decreased the amount of mAb 4/1-detectable CALEB (NMDA: 24.8%, $n = 8$; kainate: 32.0%, $n = 7$). This reduction was blocked by the receptor-specific

antagonists APV (50 μ M) or DNQX (10 μ M), respectively, either of which alone do not affect the surface expression of CALEB (Figures 1B and 1C and data not shown). Finally, we tested the contribution of voltage-activated calcium channels using a combination of L- and N-type calcium channel blockers (nimodipine, 10 μ M, and ω -conotoxin MVIIC, 1 μ M). This treatment prohibited the KCl-induced downregulation of CALEB (Figure 1C). Taken together, these observations indicate that CALEB, or a fraction of CALEB, is modulated by depolarization and calcium influx.

Depolarization Induces a Shedding of Extracellular Segments of CALEB, Thereby Exposing the EGF Domain

The rapid downregulation of cell surface-exposed CALEB in Western blots might result from a variety of mechanisms, including ectodomain shedding and/or regulation of endocytosis/exocytosis, such as that observed for TrkB (Du et al., 2003) or AMPA-type GluRs (Bredt and Nicoll, 2003). To investigate whether the regulation of endocytosis plays a role in the decrease of CALEB at the cell surface, we labeled retinal cells with a cleavable biotin reagent (NHS-SS-biotin). After KCl treatment, biotin was cleaved at the cell surface using the nonpermeant reducing agent glutathione, followed by neutralization and isolation of biotinylated proteins. Analysis of Western blots using antibodies to GluR2/3 indicated that a brief KCl treatment (10 min) increased the internalization of AMPA receptor subunits, which is consistent with published results (Kim et al., 2001; Lin et al., 2000). In contrast, internalization of CALEB was not detectable by mAb 4/1 (Figure 2A). Without glutathione-induced cleavage of the biotin, high-KCl incubation reduced, as before, the amount of the 80 kDa component of CALEB (Figure 2A, left lower panel).

In order to find out whether the downregulation was caused by shedding of the extracellular parts of CALEB, we mapped the epitope of mAb 4/1 used in the above Western blots. Several deletion constructs of CALEB fused to the human Fc-fragment and a GPI anchor attachment signal were analyzed in extracts of COS-7 cells by Western blotting using mAb 4/1 or antibodies to human Fc. On the basis of these studies, the epitope of mAb 4/1 was localized to amino acid residues 280-

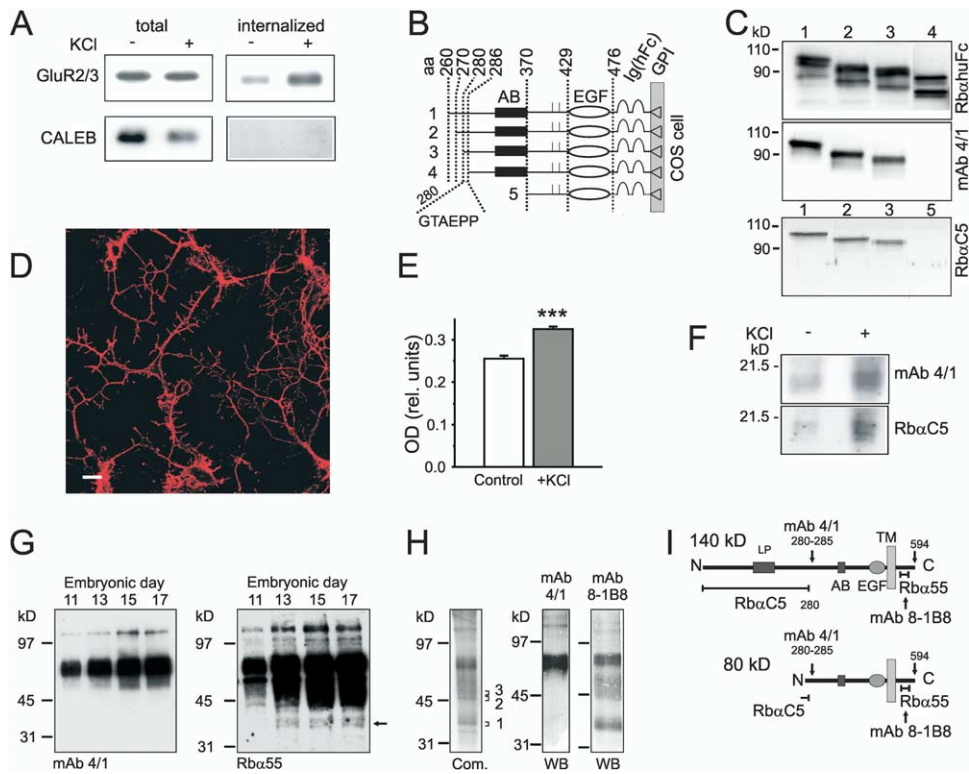


Figure 2. Ectodomain Shedding of CALEB

(A) Analysis of endocytosis of CALEB. Retinal cells were labeled with a cleavable biotin reagent (NHS-SS-biotin). In the left two lanes, CALEB and the glutamate receptor subunit GluR2/3 are compared in the presence and absence of KCl (30 mM, 10 min) without cleavage of the biotin. In the right two lanes, biotinylated internalized proteins after cleavage of cell surface biotin by a nonpermeant reducing agent are detected. This analysis using antibodies to GluR2/3 indicated that a brief KCl treatment increased the internalization of AMPA receptor, while internalized CALEB was not detectable in this assay by mAb 4/1. Lanes for internalized CALEB were exposed two times longer.

(B and C) Epitope mapping of anti-CALEB mAb 4/1 and polyclonal antibodies RbαC5.

(B) Schematic illustration of CALEB-Ig(hFc) fusion proteins expressed on COS-7 cells. The amino acid positions are given. AB, acidic box.

(C) Immunoblot demonstrating the expression of CALEB deletion constructs using antibodies to human Fc (RbαhuFc). Binding of mAb 4/1 was observed only to constructs 1-3, indicating that the epitope of mAb 4/1 corresponds to amino acid residues 280–285 of CALEB. Lanes containing constructs 1-3 were exposed for 2 s; the lane containing construct 4 was exposed for 30 s. The number of construct as indicated in (B) is given above the panel. RbαC5 was generated to affinity-purified CALEB and was observed to bind to constructs 1 to 3, but not 5.

(D) Staining of CALEB on unfixed, living retinal cells using mAb 4/1 indicated that the epitope of mAb 4/1 is exposed on the surface of cultivated cells. CALEB is localized on all neurites, including small filopodia and the soma of neurons. Scale bar, 10 μm.

(E) Cell surface bound mAb 4/1 is released upon KCl treatment (30 mM). Cultivated retinal cells were exposed to biotinylated mAb 4/1 (0.1 μg/ml). Unbound antibody was removed by washing followed by KCl treatment for 20 min. Supernatants were analyzed in streptavidin-coated ELISA plates. Note an increase of mAb 4/1 in the supernatant after KCl treatment. Error bars indicate SEM.

(F) Supernatants of retinal cultures treated without or with KCl (30 mM, 10 min) were precipitated by TCA, followed by Western blotting using mAb 4/1 or RbαC5. Note that a diffusely migrating component at 18 kDa is enriched in KCl-treated cultures that is recognized by mAb 4/1 and RbαC5.

(G) Western blot analysis of embryonic retinal tissue (E11 to E17) using mAb 4/1 or Rbα55, an antibody directed to the cytoplasmic stretch of CALEB. mAb 4/1 detected a 140 and 80 kDa band, while Rbα55 recognized several bands ranging from 63 to 38 kDa (arrow) in addition to the 140 and 80 kDa bands.

(H) Purification of CALEB from embryonic chick retinae by immunoaffinity chromatography using mAb 8-1B8, resolved by SDS-PAGE and stained by the colloidal Coomassie blue method (Neuhoff et al., 1988). The same material was blotted and analyzed by mAb 4/1 or 8-1B8. The bands that were sequenced by mass spectroscopy are indicated at the right by brackets. The following amino acid sequences were obtained: VPPPPSPTEGTPMAR, TPSELHNDNFSLSTIAEGSHPNDDPGAPHK, LQDPLKPLGLK, DEEPLSILSTAPEEGSK, GEPGGCGVPCPLHNNLG (aa position 388–594). Com., Coomassie blue; WB, Western blot.

(I) Schematic representation of the two major forms of CALEB (140 and 80 kDa) detected by mAb 4/1 in the chick retina. Epitopes recognized by the different antibodies used in these studies are indicated by arrows or a line.

285 (Figures 2B and 2C). Since mAb 4/1 binds to the surface of living retinal cells (Figure 2D), KCl-induced downregulation of CALEB might reflect the loss of the mAb 4/1 epitope from the neuronal surface. This interpretation was supported by measuring the amount of mAb 4/1 in supernatants of KCl-treated and untreated

cultures using the ELISA method. A significant increase of 27.4% ($n = 4$, $p < 0.001$) of mAb 4/1 in supernatants of KCl-treated cultures was observed, suggesting that the antibody bound to a CALEB fragment was released from the cell surface (Figure 2E).

To identify a shed CALEB component, supernatants

of KCl-treated and untreated retinal cultures were highly concentrated using TCA. mAb 4/1 detected a 18 kDa component that was elevated in supernatants of KCl-treated cultures (Figure 2F). This component was also identified by a polyclonal antibody to CALEB (Rb α C5) (Figure 2F) that binds to the N-terminal region of CALEB (see Figures 2C and 2I for the mapping). It is currently not possible to assign this shed fragment precisely to a defined amino acid region of CALEB. However, on the basis of its antibody reactivity and its migration behavior in reducing and nonreducing gels (data not shown), it might be composed of the N-terminal region of the 80 kDa form of CALEB without the EGF domain. Isolation of this shed component from embryonic retinal tissue extracts by immunoaffinity chromatography using mAb 4/1 was not successful, most likely due to its instability (see also below).

The release of an N-terminally located extracellular fragment also predicts the existence of membrane-associated truncated forms of CALEB that are not detectable by the antibodies described above (mAb 4/1 and Rb α C5). To search for such components, monoclonal as well polyclonal antibodies were generated to the cytoplasmic segment of CALEB (Rb α 55 and mAb 8-1B8; Figure 2I). These antibodies were used to analyze developing retinal tissue and to isolate the predicted truncated forms of CALEB. While mAb 4/1 stained only bands at 80 and 140 kDa (Figure 2G), antibodies to the cytoplasmic segment (Rb α 55) detected several bands smaller than the major 80 kDa, ranging from 62 to 38 kDa (arrow in Figure 2G), in addition to the 140 kDa band. These lower molecular mass components increased from E11 to E17 (Figure 2G). Molecular mass forms lower than 38 kDa were not observed in retinal tissue (Figure 2G and data not shown), suggesting that this band represents the smallest converted form. To clarify the identity of these additional bands and to assess which polypeptide modules might be present in the truncated forms of CALEB, the protein was isolated from plasma membranes of embryonic chick retinae by immunoaffinity chromatography using mAb 8-1B8. Analysis of the isolate in SDS-PAGE by Coomassie blue staining revealed molecular mass components identical to those described in the Western blotting of the developing retina. Sequencing by mass spectrometry of tryptic peptides of bands at 38, 46, or 50 kDa (marked as 1, 2, and 3, respectively, in Figure 2H, also see the legend) resulted in sequences of amino acid position from 388 to 594. The most N-terminally located peptide that was identified from the three molecular mass forms of CALEB was amino acid position 388 to 402 (VPPPPSPTEGTPMAR), suggesting that the cleavage occurred in the region between the acidic box and the EGF-like domain.

In summary, our findings indicate that the observed activity-dependent modulation of CALEB at the cell surface is the result of a shedding mechanism in the extracellular region of CALEB that, in the chick, contains the epitope of mAb 4/1. The remaining membrane-associated CALEB carries the now exposed EGF domain (see also Figure 7), which itself appears not to be released from the truncated form.

The Absence of CALEB Affects the Functional Features of Synapses at Early Postnatal but Not Mature Stages

A critical question to be answered is whether deletion of CALEB would result in a modified synaptic transmission or the development of synapses. To test this, we first compared the expression pattern between chick and mouse and investigated the putative conversion of CALEB in mouse neural tissue. As described for the chick (Schumacher et al., 1997), mouse CALEB was found to be expressed throughout the developing brain and displayed a developmentally regulated expression profile in many brain structures, including the visual system (Figure 3A). Antibodies to the cytoplasmic segment detected bands at 150 kDa, 100 kDa, and several lower molecular mass components ranging from 38 to 30 kDa in the mouse colliculus superior. Treatment with chondroitinase ABC shifts the mobility of the 150 kDa band to 100 kDa, indicating that the 150 kDa form represents the chondroitinsulfate-containing form of the 100 kDa band. In the colliculus superior, the amount of chondroitinsulfate attached to the CALEB polypeptide decreases slightly from P1 to adult, while the amount of CALEB protein increases from P1 to P22 and then decreases in the adult (Figure 3A). Within the mouse retina, CALEB was predominantly localized in the optic fiber and inner plexiform layer. In the colliculus, it displayed a more uniform distribution throughout all layers (Figures 3B and 3C). In the developing cerebellum, CALEB was primarily associated with the Purkinje cells as well as the inner granular layer (Figure 3D) (Aono et al., 2000).

Conversion of CALEB in mouse neural tissues was tested using acute postnatal brain slices—a model system known to exhibit rapid synaptic remodeling (Kirov et al., 1999; Meier et al., 2003). Slices of the colliculus superior from P3 mice were incubated for 2.5 hr with different reagents. In the presence of 2 mM calcium in artificial cerebrospinal fluid (ACSF), a significant conversion of CALEB into truncated forms of 38 to 30 kDa was observed using antibodies to the cytoplasmic segment (Figure 3E). This processing was found to be much stronger than in cell cultures from chick retinae, and it was blocked by NMDA receptor antagonists and by lowering the calcium concentration (0.1 mM) (Figures 3E and 3F). In summary, mouse CALEB reveals a similar distribution in the developing brain as chick CALEB and is also converted to smaller, membrane-attached forms. Mouse CALEB, however, differed from chick CALEB in the amount of attached chondroitinsulfate, as shown for neuroglycan C (Aono et al., 2004).

To clarify a possible role of CALEB in the development of synaptic connections in the rodent brain, we generated CALEB-deficient mice by homologous recombination. To ensure complete gene inactivation, a targeting construct was created to destroy exon 1, containing the start codon, and exon 2, which encodes the N-terminal half of the EGF domain, since the EGF domain might play a prominent role in the function of CALEB (Figure 4A). The correct integration of the targeting vector and deletion of exons 1 and 2 were confirmed by Southern hybridization as shown in Figure 4B using the fragment obtained by digestion with HindIII. The replacement of the half EGF domain by the

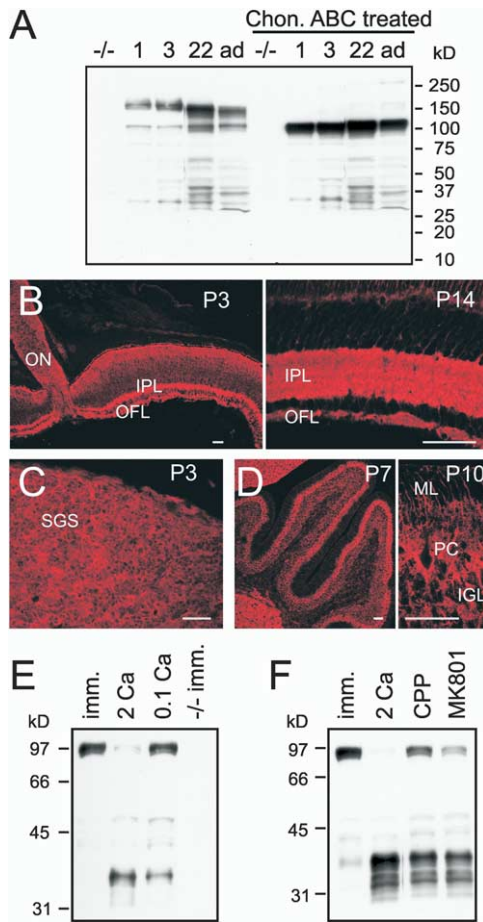


Figure 3. Characterization of CALEB in Mouse Neural Tissue
(A) Western blot analysis of different developmental stages of the colliculus superior (P1, 3, and 22) using an antibody to the cytoplasmic domain of CALEB (Rb α 55). Samples were untreated or treated with chondroitinase ABC. ad, adult. (B) Expression of CALEB in cryostat sections of the developing retina using immunocytochemistry (Rb462). Note a strong localization of CALEB in the IPL. (C) Expression of CALEB in the colliculus superior at P3 (Rb α 55) and in the (D) developing cerebellum at P7 and P10 (Rb462). IGL, internal granular layer; IPL, inner plexiform layer; ML, molecular layer; ON, optic nerve; OFL, optic fiber layer; PC, Purkinje cells; SGS, stratum griseum superficiale. Scale bar, 50 μ m. (E and F) CALEB is converted to truncated forms in the presence of calcium, which can be blocked by lowering the calcium concentration and by NMDA receptor antagonist (MK801 20 μ M, CPP 100 μ M). Acute slices from P3 mice were incubated in ACSF with the reagents indicated above the panel for 2.5 hr or were immediately processed for Western blotting (imm.). Proteins were analyzed by Western blotting after chondroitinase ABC treatment using Rb α 55. For demonstrating the specificity of the antibodies, the colliculus superior from CALEB-deficient mice is also shown.

neo cassette in the mutant mice was verified by PCR (Figure 4C). Western blots from brains of early postnatal stages revealed the absence of CALEB polypeptides (Figure 4D). CALEB knockout mice were then bred from a mixed genetic background to a pure C57BL/6J background. Breeding of heterozygotes deviated slightly from the expected Mendelian ratio (29% +/+, 42% +/-, and 29% -/-; n = 185), but indicated that knockout

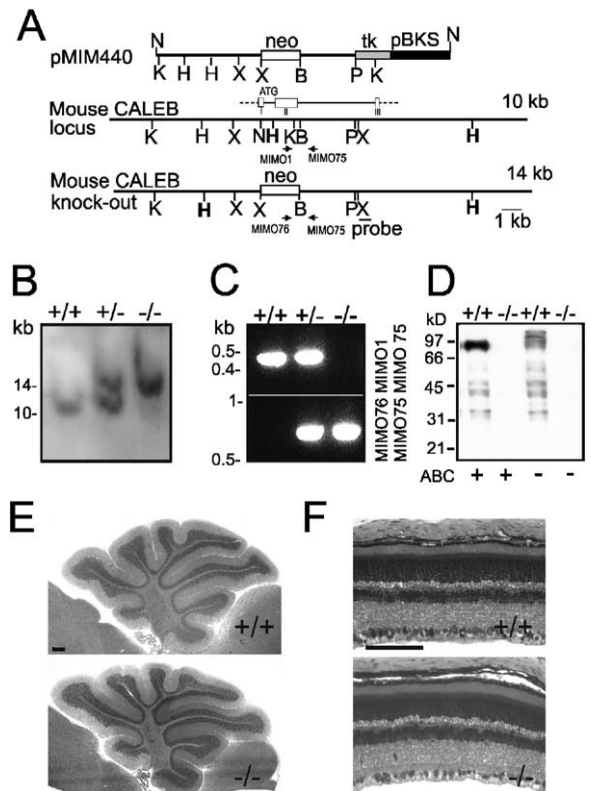


Figure 4. Generation of CALEB-Deficient Mice
(A) Map of the targeting vector and of part of the genomic locus before and after homologous recombination with the targeting vector. The position of exons is indicated. neo, PGKneopA cassette; tk, MC1TKpA cassette. Relevant restriction sites are indicated as follows: B, BamHI; H, HindIII; K, KpnI; P, PstI; and X, XhoI. The positions of the external Southern blot probe as well as the PCR primers are indicated. (B) Southern blot of DNA from tail biopsies of wild-type, heterozygous, and homozygous mice, using the restriction enzyme HindIII. (C) PCR genotyping using primers MIMO1 and MIMO75 for the wild-type reaction (no band in the preparation from the knockout mouse) and MIMO76 and MIMO75 for the knockout reaction (no band in the preparation from the wild-type mouse). (D) Immunoblot analysis using extracts of whole brains from wild-type and CALEB-deficient mice deglycosylated by chondroitinase ABC or untreated using a polyclonal antibody against the cytoplasmic segment of CALEB (Rb α 55). CALEB bands are completely absent in the mutants. The absence of CALEB was also demonstrated by antibodies to the extracellular part of CALEB (Rb α 462) (data not shown). Molecular mass markers are indicated to the left of the panel. (E and F) The CALEB-deficient mice do not reveal any gross anatomical defects. Shown are Toluidine blue-stained cryostat sections of the cerebellum (P20) and the retina (P20). Scale bar, 100 μ m (E), 50 μ m (F).

animals survive with the same rate as wild-type animals. The analysis of the body weights of CALEB-deficient mice during postnatal development revealed no difference compared to control C57BL/6J mice. However, the mutants were found not to care for their litters as well as the wild-type mice, suggesting a deficit in maternal behavior (data not shown). Morphological investigations of brains of mice lacking CALEB using toluidine blue stain or labeling with antibodies directed to

a variety of neural proteins failed to uncover structural abnormalities in brain architecture (Figures 4E and 4F and data not shown).

To examine the synaptic connectivity, we applied whole-cell patch-clamp techniques to record pharmacologically separated excitatory and inhibitory postsynaptic currents (EPSCs, IPSCs) in acute horizontal slices of the superficial (visual) layers of the colliculus superior from wild-type and CALEB-deficient mice. Since CALEB is developmentally regulated (see Figure 3A), recordings were made from two different stages, postnatal day 1–3 (P1–3) and postnatal day 20–22 (P20–22), representing stages of synapse immaturity and maturity (Juttner et al., 2001). To ensure a reasonable yield of events at the early stage, spontaneous postsynaptic currents (sPSCs) were acquired instead of miniature PSCs. Quantitative analysis of spontaneous synaptic currents revealed that in the younger age group (P1–3) the sPSC frequency was significantly lower in the absence of CALEB (Figures 5A, 5B, 5D, and 5E). Specifically, the frequency of sEPSCs was 0.0122 ± 0.0021 Hz (21 cells, 9 animals) in the knockout and 0.0258 ± 0.0045 Hz (22 cells, 9 animals, $p < 0.004$) in the wild-type mice. Spontaneous IPSCs had a frequency of 0.039 ± 0.009 (28 cells, 6 animals) for the knockout and 0.090 ± 0.025 (24 cells, 8 animals, $p < 0.04$) in wild-type slices. Interestingly, no significant differences were observed at more mature stages (P20–22). The mean amplitudes and decay time constants of sIPSCs in knockout mice were not statistically different from those in wild-type mice at either age (Figures 5C and 5F and data not shown). Similar observations regarding the frequencies, amplitudes, and decay time constants of PSCs were obtained on a mixed genetic background (Sv129/Bl6) (data not shown). To exclude the possibility that the reduced PSC frequency resulted from an altered action potential generation, we recorded voltage-gated Na^+ and K^+ currents and calculated the respective current densities. However, no differences were found in this regard between wild-type and knockout mice. Likewise, repetitive spike discharge in response to depolarizing current pulses was also found to be unchanged by the absence of CALEB (data not shown).

The Absence of CALEB Results in a Lower Release Probability of Immature GABAergic Synapses

The difference in the sEPSCs and sIPSCs frequency and the lack of changes in the amplitude and decay time of postsynaptic currents point to a decreased number of synapses and/or alterations on the presynaptic side. To distinguish between these possibilities, the number of synapses was counted in electron microscopic view fields in sections prepared from the colliculus superior at P3. In mutant mice, synapses appeared to be structurally normal and occurred at the same number as in the wild-type colliculus (Figures 5G and 5H). Also, no difference between wild-type and knockout was observed when electron microscopic images were obtained from slices incubated for 2.5 hr in ACSF (data not shown). To provide independent evidence for these observations, additional counts were performed at the light microscopic level. Sections from P3 superior colliculus were stained by antibodies directed to

the vesicular transport proteins VIAAT and VGlut I-II that allow us to distinguish between GABAergic/glycinergic and glutamatergic terminals, respectively. Again, the number of excitatory as well as inhibitory spots remained at the same level as in wild-type animals (Figures 5I and 5J), suggesting that the absence of CALEB does not influence synapse numbers.

To characterize presynaptic features of synapses in CALEB-deficient mice, we performed paired-pulse experiments, a commonly used approach to determine presynaptic function. Since at P1–3 the rate of occurrence of sIPSCs (wild-type: 80.0%, 24 of 30, and knockout: 84.8%, 28 of 33) was higher than that of sEPSCs (wild-type: 61.1%, 22 of 36; knockout: 69.4%, 25 of 36), the following tests were confined to GABAergic connections. Paired-pulse experiments were performed by applying two pulses at 20 ms and 100 ms intervals at maximal electrical stimulation in the vicinity of the tested postsynaptic neuron. At both intervals, a significantly higher paired-pulse ratio in CALEB-deficient mice was observed. Again, no difference was found between knockout and wild-type mice at an older age (Figures 6A and 6B). Consistent with these observations on paired-pulse properties, we found lower amplitudes of the evoked IPSC in knockout preparations from P1–3 mice, but not at P20–22 mice (Figure 6C).

Further data in support of the notion that CALEB deficiency results in an alteration of transmitter release were obtained in tests with high-frequency stimulation at maximal intensity. Figures 6D and 6E illustrate that at P1–3 inhibitory synapses in CALEB-deficient mice displayed less depression in the course of a prolonged high-frequency activation (10 pulses, 50 Hz). Again, this resistance to depression in knockout mice was not detectable at P20–22 (Figure 6F).

The higher paired-pulse ratio and the reduced depression of postsynaptic responses during repetitive stimulation in CALEB-deficient mice are consistent with a lower release probability (P_r). To determine P_r and the size of the readily releasable vesicle pool (RRP), neurons were stimulated at 50 Hz (40 pulses). Again, the amplitudes of the first eIPSCs in each test response were lower in knockouts as compared to wild-type preparations (Figure 6G). However, in contrast to wild-type preparations, eIPSCs in CALEB-deficient preparations displayed an initial facilitation, followed by a gradual decrease to a steady-state level. To obtain an estimate of the RRP, the cumulative quantal content was plotted against stimulus number (Figure 6H). The quantal content (i.e., the number of vesicles released with each consecutive stimulus) was obtained by dividing the eIPSC amplitude by the amplitude of the quantal inhibitory postsynaptic current (q_{IPSC}). The q_{IPSC} was defined for each tested cell as the first peak in the amplitude distribution of the delayed IPSCs produced after the end of the high-frequency stimulus trains (Figure 6H, insert; for more details, see Kirischuk et al., 2005). The average value of q_{IPSC} was 15.91 ± 0.79 ($n = 16$) in wild-type preparations and 14.66 ± 0.58 ($n = 17$) in knockout preparations. The difference was not significant. The RRP of the synchronous release was estimated by back-extrapolation from the linear portion of the curve to the y axis intercept. The y-intercept gives the total release minus the total replenish-

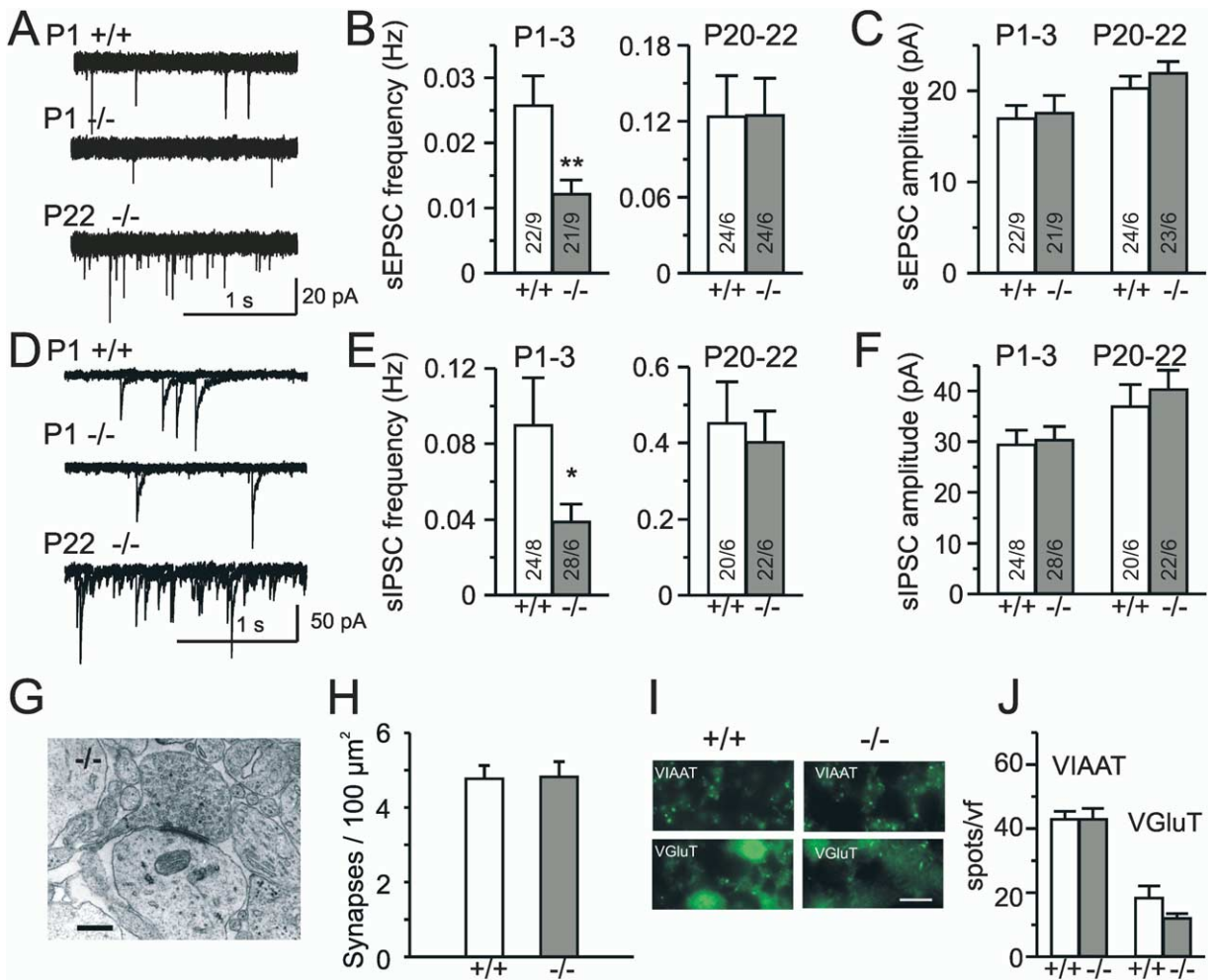


Figure 5. Spontaneous Frequencies of EPSCs and IPSCs Are Reduced in CALEB-Deficient Mice at Early Postnatal but Not Mature Stages, while Synapse Numbers Remained Unchanged

(A and D) Specimen recordings of spontaneous synaptic activity in acute slices of the colliculus superior at two different developmental stages: P1–3 and P20–22. sEPSCs were recorded in the presence of bicuculline (20 μM), and sIPSCs were recorded in the presence of DNQX (10 μM) and APV (50 μM). Holding potential, –70 mV.

(B, C, E, and F) Quantification of results, mean and SEM. Note differences in sPSC frequency but not in the amplitude. The numbers within the columns indicate the number of cells and animals analyzed. Error bars indicate SEM. **p < 0.01, *p < 0.05.

(G–I) Analysis of synapse numbers by electron microscopy and immunofluorescence of presynaptic proteins in the colliculus superior at P3 in wild-type and mutant mice.

(G) CALEB-deficient synapses appear indistinguishable from wild-type synapses. Scale bar, 0.5 μm.

(H) The number of synapses within the colliculus superior is not affected by the absence of CALEB. Average number of synapses were obtained from 487 electron microscopic fields/6 animals and 455 fields/8 animals from wild-type and CALEB-deficient mice, respectively. Error bars indicate SEM.

(I and J) Comparison of slices from P3 wild-type and knockout mice reveals no changes in the presynaptic expression of VIAAT or VGluT 1+II puncta. Scale bar, 10 μm.

(J) Number of spots of the presynaptic vesicle proteins VIAAT or VGluT per microscopic view field (vf) are given (n = 4–8). Error bars indicate SEM.

ment, which can be viewed as an estimate of RRP. The RRP value calculated by this method was 119.6 ± 17.9 vesicles (n = 16) and 98.8 ± 14.9 vesicle (n = 17) for wild-type and CALEB knockout mice, respectively. The difference between the two genotypes was not significant. Having an estimate of RRP, P_r could be calculated as $P_r = eIPSC1/(RRP \times q_{IPSC})$. The estimated values of P_r were 0.293 ± 0.022 for wild-type (n = 16) and 0.193 ± 0.023 (n = 17) for knockout mice. This difference was significant at p < 0.01 (Figure 6I).

Considering these differences in P_r , we searched for quantitative changes in the fine structure of presynaptic terminals by performing a double-blind morphometric analysis of EM images obtained from the P3 colliculus superior. In these measurements, we detected no significant difference in the number of docked vesicles per micrometer of active zone or the fraction of docked vesicles, indicating that the absence of CALEB does not lead to an overall remodelling of presynapses (Table 1). We then analyzed vesicle-enriched synaptosomal

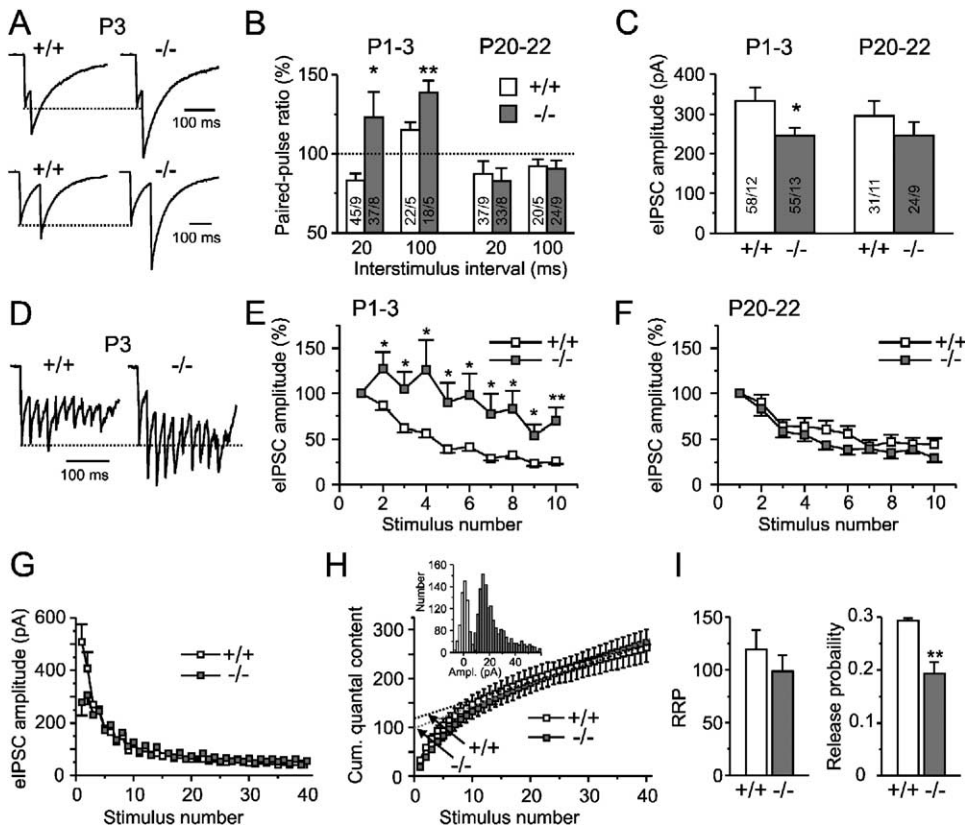


Figure 6. CALEB Deficiency Affects Presynaptic Properties at Early Developmental Stages

(A) Specimens of eIPSCs during a paired test at interstimulus intervals of 20 ms and 100 ms. Averaged traces ($n = 10$) from wild-type and CALEB-deficient mice at P3. The first amplitudes were normalized to 1.

(B) Quantification of the results from paired-pulse tests. Ten to twenty trials per interval. The paired-pulse ratio (PPR) is determined from averaged traces as $(\text{eIPSC2}/\text{eIPSC1}) \times 100$. Note that at P1–3 the PPR is different in wild-type and CALEB-deficient mice. Differences between the two groups are significant at both interstimulus intervals ($*p < 0.05$, $**p < 0.01$). Error bars indicate SEM.

(C) Comparison of evoked amplitude of eIPSCs from wild-type and mutant mice at P1–3 and P20–22. Error bars indicate SEM.

(D) Specimen records to show responses to high-frequency activation.

(E and F) Quantification of the results obtained with high-frequency stimulus trains (10 pulses, 50 Hz). eIPSC amplitudes were normalized to the eIPSC amplitude after the first stimulus. Note that CALEB-deficient mice display less depression during the ten trials. The second response is larger than that of the first one. Significance levels apply to the comparison between wild-type and CALEB-deficient mice at P1–3 ($p < 0.05$). Error bars indicate SEM.

(G) Quantification of results obtained with longer stimulus trains (40 pulses, 50 Hz) at P3. Note lower initial amplitudes in CALEB-deficient mice.

(H) Cumulative plot of average quantal content. Data points represent averaged responses from 16 wild-type neurons and 17 knockout neurons. A linear regression curve was fitted to the data points obtained for the 15th to 40th stimulus. The y-intercept was back-extrapolated from the linear regression curve. Intercepts provide an estimate of RRP. The insert represent an amplitude distribution of IPSCs of CALEB-deficient mice, obtained from the delayed release (in gray, 1134 events), and of background noise (white, both bin sizes = 2 pA). Error bars indicate SEM.

(I) Summary results of readily releasable vesicle pool (RRP) and release probability (P_r). P_r was calculated as $\text{eIPSC1}/(\text{RRP} \times q_{\text{IPSC}})$. Error bars indicate SEM.

preparations from P3 colliculi superior by biochemical methods (Huttner et al., 1983) and surveyed several presynaptic proteins, including those that are known to affect P_r or PPF if absent, such as Rab3A (Geppert et al., 1994), Rab-GDI (Ishizaki et al., 2000), synapsin I (Rosahl et al., 1995), RIM1 (Schoch et al., 2002), and calcium sensor synaptotagmin1 (Fernandez-Chacon et al., 2001). Of the 18 proteins tested (synapsin I, synaptophysin, synaptobrevin 2, synaptotagmin1, Rab-GDI, α -NSF, α -rabphilin, SNAP-25, SNAP-23, rab 3A, rab 5, α -synuclein, RIM-1, calbindin, calretinin, parvalbumin, VIAAT, and VGlut I+II), none showed a change in expression in the two compartments analyzed: LS2 (synaptosomal supernatant) and LP2 (crude synaptosomal

pellet) (see Figure S1 in the Supplemental Data available with this article online).

In summary, the absence of CALEB altered synaptic transmission, and its regulation might provide a molecular basis for maintaining normal release probability at early postnatal stages.

Discussion

Modification of the Molecular Structure of CALEB by Neuronal Depolarization and Calcium Influx

Our aim was to identify cell surface proteins that are modulated by neural activity and expressed during periods of active synaptogenesis. Such proteins might

Table 1. Quantitative Ultrastructural Analysis of Synapses of Colliculus Superior from P3 Wild-Type or CALEB-Deficient Mice

	Wild-Type	CALEB Knockout
Number of synaptic profiles counted	45	53
Synaptic cleft (nm)	21.1 ± 0.5	21.4 ± 0.7
Vesicle diameter (nm)	39.4 ± 0.7	39.8 ± 0.7
Docked vesicles per μm active zone	15.9 ± 1.0	15.6 ± 0.9
Docked vesicles/total number of vesicles (%)	15.2 ± 1.0	16.2 ± 1.4
Total number of synaptic vesicles per μm ² of presynaptic terminal	75.0 ± 4.7	76.5 ± 5.2

Values are mean ± SEM.

have a function in synapse formation and/or plasticity. In this study, we report that the conversion of CALEB is facilitated in an activity-dependent manner. The modification becomes detectable after a relatively short time period of 10 min, can be induced by elevated KCl and glutamatergic transmitter receptor agonist, and can be specifically blocked by receptor antagonists and by L- and N-type calcium channel blockers. This processing occurs at the plasma membrane and results in a truncated membrane-associated form of CALEB with an exposed EGF domain with a molecular mass of 38 kDa (see scheme in Figure 7). Different intermediate processing products are generated in different cell types. These observations were made in the chick and mouse. Based on the amino acid sequences determined from the converted form, the site of processing might be between the acidic box and the EGF-like domain of CALEB.

The EGF domain is likely to play a prominent role in the function of CALEB and becomes accessible upon processing for interaction with a yet unknown receptor,

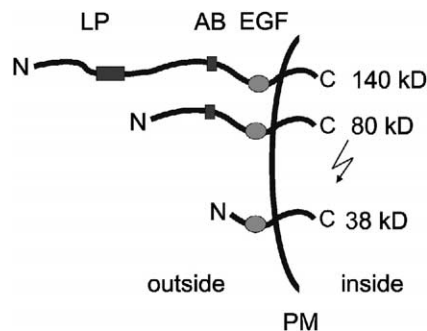


Figure 7. Proposed Model for Activity-Dependent Conversion of CALEB

Unprocessed CALEB is expressed as plasma membrane polypeptide (in chick retina as a 140 kDa form) that is processed in an activity-dependent manner, resulting in a transmembrane form composed of the EGF domain, the transmembrane region, and the cytoplasmic segment. A prominent intermediate form in the chick retina is the 80 kDa component, which is further processed. Different intermediate processing products exist in different cell types. It cannot be completely excluded that the EGF domain is also released (see Discussion). AB, acidic box; LP, leucine, proline-rich region; PM, plasma membrane.

such as ErbB3 as proposed for neuroglycan C (Kinugasa et al., 2004), or a ligand provided by neighboring neurons. In this scenario, CALEB might function as an activity-dependent juxtacrine signaling system, and its regulation might provide a molecular basis for activity-dependent synaptic plasticity at early stages. In addition, the processing disrupts interactions of the more N-terminal regions of CALEB with tenascin-R, tenascin-C (Schumacher et al., 2001; Schumacher and Stube, 2003), or other as yet unknown proteins. Identification of a putative receptor protein of the EGF domain might help to distinguish between these two possibilities and may help to explain more precisely how neural activity modulates the molecular interactions of CALEB. Currently, we cannot completely exclude a release of the EGF domain from the truncated transmembrane form. However, we consider this as unlikely for two reasons: (1) smaller components containing only the cytoplasmic segment of CALEB were not detected in neural tissues by antibodies to the cytoplasmic segment of CALEB; and (2) the stalk region between the EGF domain and the transmembrane segment of CALEB (4–6 amino acid residues) is too short for a release of the EGF domain by a protease at this site. The proteolytic release of the EGF domain of the related neuregulin-1 requires a minimum length of 11 amino acid residues of the stalk stretch between the EGF domain and the transmembrane segment (Han and Fischbach, 1999). However, alternative proteolytic processing pathways within the transmembrane region leading to a release of the EGF domain are also conceivable (Urban et al., 2002).

Altered Synapse Function at Early Postnatal Stages in the Absence of CALEB

As a first step toward characterizing the role of CALEB in synapse formation, we compared features of synapses in CALEB-deficient and wild-type neurons at different developmental stages. Although mice lacking CALEB did not exhibit an overt phenotype in the adult, electrophysiological analysis of synaptic connectivity in the visual layers of the colliculus superior demonstrated that specific aspects of synaptic transmission are altered in the mutant mice. At the outset, it is important to note that all measured effects of CALEB gene inactivation were confined to a very young age when glutamatergic synaptogenesis starts and most GABAergic synapses are still depolarizing in the colliculus superior (Grantyn et al., 2004). In the absence of CALEB, four observations were made: (1) the frequency of spontaneous EPSCs and IPSCs was lower, (2) the paired-pulse ratio was higher, (3) the depression of evoked IPSCs during high-frequency stimulus trains was lower, and (4) the neurotransmitter release probability was lower. The number of synapses in the colliculus superior, as well as the decay time constants of postsynaptic currents, remained unchanged. The lower P_r in the absence of CALEB was not accompanied by a change in the size of docked vesicle fraction or in the level of presynaptic proteins. The molecular nature of the process accounting for the CALEB dependency of P_r therefore remains to be determined.

It is nonetheless conceivable that CALEB normally functions in the processes of the assembly of syn-

apses. Deletion of CALEB could then lead to a change in synaptic transmission as observed here. It has become clear that a high level of P_r must be regarded as a characteristic feature of immature synapses (Bolshakov and Siegelbaum, 1995; Mozhayeva et al., 2002). A high efficacy of transmitter release ensures a high level of local depolarization and calcium elevation in response to a presynaptic action potential, and this is considered to be a prerequisite for postsynaptic receptor accumulation, both at glutamatergic and at GABAergic sites. It is currently unknown whether CALEB is expressed on the pre- or postsynaptic side or on both. Independent of the precise mechanism of action of CALEB, our experiments reveal that CALEB is implicated in the development of the presynapse by affecting the release probability. Therefore, it can be suggested that CALEB performs an essential role during early stages of brain development.

CALEB is restricted to the nervous system; in the mouse it contains high amounts of chondroitinsulfate and is highly expressed during so-called critical periods when the developing brain is very plastic and strongly reacts to environmental signals (our unpublished data). In contrast to our previous *in vitro* antibody perturbation experiments (Schumacher et al., 1997), there was no evidence for reduced axon extension and filopodial outgrowth in the mutant mice or in neuronal cultures from CALEB-deficient mice (our unpublished results). *In vivo* CALEB appears to be required for the function of synapses within a limited time window, or it might be important for the fine-tuning during the early phases of circuit formation. The absence of an overt phenotype in adult CALEB-deficient mice suggests that other mechanisms can compensate for this protein in these mice or that CALEB might be important only during the process of synapse maturation. However, it is currently unknown whether this impairment of synapse function in the absence of CALEB is accompanied by a permanent change in sensory function of the adult nervous system. It has widely been assumed that connections between pre- and postsynaptic neurons are strengthened or weakened by mechanisms that are able to interpret patterns of neural activity (Berardi et al., 2003; Hensch, 2004) and that involve chondroitin-sulfate-containing proteins (Pizzorusso et al., 2002). The influence of neuronal activity on the synapse development in the nervous system is most obvious under competitive experimental conditions. Therefore, a further characterization of the activity-dependent processing of CALEB might be obtained by developing genetic models in which CALEB-positive and -negative neurons are simultaneously available within one region of the developing brain. In such a competitive situation, it might be possible to test whether CALEB-deficient neurons are less successful in generating and maintaining synapses in comparison to wild-type neurons.

Experimental Procedures

Retinal Cultures, KCl Treatment, Biotinylation, and ELISA

Retinal cells from 8-day-old chick embryos (E8, white leghorn) were cultivated on poly-L-lysine (100 μ g/ml, Sigma) coated dishes at a density of 1.7×10^6 cells/ml/well of a 24-well cluster in DMEM supplemented with N2 (GIBCO). After 3 days *in vitro*, cultures were

treated for different time intervals with 30 mM KCl, 10 μ M NMDA, or 50 μ M kainate in DMEM/N2 or were kept in DMEM/N2. Blockers (APV, DNQX, and nimodipine, all from Tocris; ω -conotoxin MV1C, Sigma) were added simultaneously with or without agonist. Cells were then washed two times with ice-cold HBSS (GIBCO), and cell surface proteins were biotinylated with EZ-link Sulfo-NHS-LC-Biotin (Pierce, 0.5 mg/ml, for 40 min at 4°C) in HBSS followed by two washes with ice-cold HBSS (GIBCO) and quenching in DMEM for 10 min at room temperature. After lysis with ice-cold 1% n-octylglucoside (Roche) in PBS supplemented with protease inhibitors (aprotinin, leupeptin, pepstatin, and PMSF) for 10 min, biotinylated proteins were captured using 12 μ l of a streptavidin bead suspension (Pierce) followed by two washes in PBS and elution by SDS-PAGE sample buffer. In the initial screen to identify activity-dependent modulated cell surface proteins, retinal cells were directly analyzed by Western blotting without biotin labeling. Binding of primary antibodies was detected with appropriate secondary antibodies (Dianova) using chemiluminescent peroxidase substrate (Pierce) or alkaline phosphatase color reaction. Band intensities were quantified by ImageJ software (NIH) and were normalized to the control level.

For the analysis of surface internalization of proteins, retinal cells were treated essentially as described by Lin et al., 2000.

For the identification of shed fragments, retinal cells were plated at a higher density, as described above ($1-1.4 \times 10^8$ cells/14 cm dish) and were cultivated for 3 days *in vitro*, followed by treatment with KCl (30 mM) in DMEM/N2 for 10 min or were kept untreated. Supernatants supplemented with protease inhibitors were clarified by centrifugation at $16,100 \times g$, followed by $100,000 \times g$ for 15 min each. Supernatants were precipitated with 1/10 vol TCA, washed twice with 95% ethanol, air dried, and resuspended in SDS-PAGE sample buffer.

For the estimation of released mAb 4/1 from cultivated retinal cells, mAb 4/1 was biotinylated by NHS-biotin. Retinal cells were incubated with biotinylated mAb 4/1 (0.1 μ g/ml, 30 min) and unbound mAb 4/1 was washed out. Supernatants of retinal cells treated with or without KCl were incubated in ELISA plates pre-coated with streptavidin (1 μ g/ml) overnight. Captured mAb 4/1 was detected by rabbit anti-mouse coupled to HRP and O-phenylenediamine as chromophore.

Antibodies, cDNA Constructs, Deglycosylation, Amino Acid Sequencing, Preparation of Crude Synaptic Vesicles, and Sequencing of Tryptic Peptides

mAb 4/1 and rabbit antibodies to the immunoaffinity isolate of CALEB (Rb α C5) have been described previously and were used in Western blots at a concentration of 0.06 μ g/ml or 3 μ g/ml, respectively (Schumacher et al., 1997). Polyclonal antibodies to the extracellular region of mouse CALEB (Rb α 462) were generated in rabbits to a His-tagged fusion protein containing amino acid regions 48 to 420 using pQE-30 (Qiagen). The IgG fraction was affinity purified on the mouse CALEB fusion protein immobilized on nitrocellulose and used at a concentration of 1 μ g/ml. Polyclonal antibodies to the cytoplasmic segment of CALEB (Rb α 55) were generated to a synthetic peptide [(C)SLSTIAEGSHPNDDP-amide] coupled to key-hole limpet hemocyanin. Antibodies were purified on the peptide AEGSHPNVRKFC coupled to N-hydroxysuccinimide-activated Sepharose (Amersham Biosciences) and eluted by a pH gradient from pH 5.0 to pH 3.0. The fraction eluting at pH 3.5 to pH 3.0 was used in Western blots at a concentration of 60 ng/ml. mAbs to the cytoplasmic segment of CALEB were generated to the above mentioned peptide as described (Rathjen et al., 1987). mAbs to F11 (contactin1) and NgCAM (chick L1) have been detailed elsewhere and were used at 1 μ g/ml (Rathjen et al., 1987). mAb anti- γ -tubulin and anti-FLAG mAb M2 (both Sigma) were diluted as recommended by the supplier. Rabbit polyclonal antibodies to the human Fc-fragment and rabbit antibodies to the glutamate receptor GluR2/3 (a gift from L.R.G. Britto) were used at 1 μ g/ml and 1:500, respectively. The guinea pig anti-VIAAT (Dumoulin et al., 1999) was applied at 1:800 and guinea pig anti-VGluT I-II (Herzog et al., 2001) at 1:500 (gift from S. El Mestikawy). Lysates were deglycosylated by chondroitinase ABC (Sigma) at a concentration of 0.02 units per 1 mg of protein (15 min, RT). For sequencing of CALEB peptides,

CALEB was isolated from detergent extracts of plasma membrane preparations of E15 chick eyes by mAb 8-1B8 immunoaffinity chromatography using procedures as detailed elsewhere (Schumacher et al., 1997). Polypeptides were separated by SDS-PAGE, and bands were excised, alkylated, and digested by trypsin. Peptides were sequenced by mass spectrometry using a nano-electrospray hybrid quadrupole spectrometer Q-ToF (Micromass) (Steen and Mann, 2004). The Mascot software package (Matrix Science) was used for data evaluation.

Crude synaptic vesicles were prepared from P3 colliculi superior of wild-type and CALEB-deficient mice following the procedure described in Huttner et al., 1983.

Mapping the CALEB Locus and Derivation of Mutant Mice See the Supplemental Data.

Immunohistochemistry

Coronal slices (500 μm) of the colliculus were fixed in 4% (w/v) paraformaldehyde and 4% (w/v) sucrose in PBS for 6 hr at 4°C, washed three times in PBS, and cryoprotected overnight at 4°C in PBS containing 8% sucrose. Slices were subsequently embedded in Tissue-Tek OCT compound (Sakura Finetek, AT Zoeterwoude, Netherlands), and 20 μm sections were cut using a cryomicrotome (Jung CM 1800, Leica). Sections were processed for immunocytochemistry as follows: after three washes in PBS, sections were washed once in PBS containing 0.1% (w/v) gelatin and incubated overnight at 4°C in a humid chamber with primary antibodies diluted in PBS/gelatin, supplemented with 0.12% (w/v) Triton X-100. After extensive washes in PBS/gelatin, secondary antibodies were applied for 1 hr at RT. To rule out unspecific binding, primary antibodies were replaced by similarly diluted normal serum from the same species. $90 \times 68 \mu\text{m}$ view fields were chosen randomly, and images were acquired (at 1000 \times magnification) using a 12 bit cooled digital camera (Photometrics, Tucson, AZ) mounted on an epifluorescence microscope (Axiovert, Zeiss, Oberkochen, Germany). Appropriate fluorescence filter sets were purchased from Omega Optical Inc., Brattleboro, VT.

For quantification of immunoreactivity, CCD images were thresholded using NIH image software to define clusters and to avoid coalescence of immunoreactivity (Meier et al., 2003; Meier and Grantyn, 2004). The number and surface area of VIAAT and VGluT clusters were derived from 25 to 50 view fields (3 to 6 independent experiments each).

Electron Microscopy

Superior colliculi were fixed with 2.5% glutaraldehyde/2% formaldehyde in 0.1 M sodium cacodylate buffer (pH 7.4) and 3 mM CaCl_2 for 24 hr at 4°C and were postfixed with 1% OsO_4 in cacodylate buffer for 2 hr, dehydrated in a graded ethanol series and propylene oxide, and embedded in Poly/Bed[®] 812 (Polysciences, Inc.). Horizontal ultrathin serial sections (75 nm) from the ventral half of the visual layer were contrasted with uranyl acetate and lead citrate and analyzed in a LEO 910 electron microscope. Ten photos per section were taken randomly at a primary magnification of 10,000 \times , and the number of synapses per area was counted on photographs at a magnification of 20000 \times . To avoid counting the same synapse twice, 20 sections (about 1.5 μm) were discarded between sections to be analyzed within one series. Profiles were identified as synapses when apposed membranes occurred closely together, with an electron-dense paramembranous specialization on one or both sides of the intervening cleft, and the presence of three or more vesicles in the vicinity of the region of apposed membranes in the presumptive presynaptic profile. All together, 487 and 455 fields were counted from six wild-type and eight CALEB-deficient mice, respectively. One field represented 57.7 μm^2 . For quantification of the synaptic profiles, the photographed synapses were calculated by Soft Imaging System software (analySIS). The area of the presynaptic terminal, the length of the active zone, the diameter of synaptic vesicles, and the size of the synaptic cleft were calculated in 45 and 53 synapses from wild-type and CALEB-deficient mice, respectively. The diameter of the synaptic vesicles was taken as the diameter of a circle. Only vesicles that were completely visible were included. Vesicles touching directly the presynaptic mem-

brane or within 40 nm of it were included in the morphological estimate of docked vesicles.

Electrophysiology

Horizontal slices of the superior colliculus (SC) from pigmented mice (C57Bl/6J) and CALEB knockout mice were prepared as described (Juttner et al., 2001). Briefly, mice were anesthetized and decapitated at two ages: P1–3 and P20–22. After dissection of the dorsal midbrain in ice-cold ACSF, two horizontal slices comprising the visual layers of the colliculus superior were obtained by vibratome cutting (150 μm). During recordings, slices were perfuse at a flow rate of 2 ml/min with ACSF consisting of 125 mM NaCl, 4 mM KCl, 10 mM glucose, 1.25 mM NaH_2PO_4 , 25 mM NaHCO_3 , 2.0 mM CaCl_2 , and 1.0 mM MgCl_2 .

The recording pipette solution contained 120 mM KCl, 4 mM NaCl, 5 mM ethylene glycol-bis(β -aminoethyl ether) N,N,N',N'-tetraacetic acid (EGTA), 10 mM N-2-hydroxyethylpiperazine-N'-2-ethanesulfonic acid (HEPES), 0.5 mM CaCl_2 , and 4 mM MgCl_2 and was buffered to pH 7.3.

Postsynaptic currents were isolated pharmacologically by blocking glutamatergic input (DNQX, 10 μM ; DL-APV, 50 μM) or by blocking GABAergic input (bicuculline methiodide, 20 μM). Evoked inhibitory postsynaptic currents were induced by blind extracellular stimulation (10 μA , 0.5 ms) through a glass pipette filled with bath solution. The stimulation rate was selected low enough to ensure recovery of the presynaptic terminals from the previous stimulation (intersweep interval 30 s). Recordings were made using an EPC-9 and were sampled at a rate of 10 kHz (WinTida, HEKA Electronics, Germany). Postsynaptic currents were filtered at 3 kHz and were analyzed offline using MiniAnalysis (Synaptosoft). In repetitive stimulation experiments, trains of pulses were applied (10 or 40 pulses, 50 Hz). Each stimulation train was repeated at least ten times. The period between successive trains was 1 min. The asynchronous IPSC amplitudes provide an estimate for quantal size.

Numerical data are reported as means \pm SEM. Statistical analysis was performed using StatView (SAS Institute Inc.). Mann-Whitney U test was used for statistical comparisons.

Significance levels are indicated as * $p < 0.05$, ** $p < 0.01$, and *** $p < 0.001$.

Supplemental Data

The Supplemental Data that accompanies this article can be found online at <http://www.neuron.org/cgi/content/full/46/2/233/DC1/>.

Acknowledgments

We thank Yvonne Klosovsky and Frank-Peter Kirsch for technical help, and Thomas Brümmendorf (Basel) for the DELF vector. We thank Frank Pfrieger for discussions at initial stages of the project on the activity-dependent regulation of neural proteins. We acknowledge the critical reading of our manuscript by Ralf Schneggenburger (MPI Göttingen, Göttingen). We thank Helmut Kettenmann for sharing electrophysiological equipment and S. El Mestikawy, B. Gasnier, and L.R.G. Britto for antibodies. These studies were supported by a Deutsche Forschungsgemeinschaft grant SFB 515 to F.G.R. and to R.G., by a predoctoral fellowship of the DFG to D.D., and by a Liebig stipend of the Fonds der chemischen Industrie to M.I.M.

Received: March 1, 2004

Revised: January 14, 2005

Accepted: February 27, 2005

Published: April 20, 2005

References

- Aono, S., Keino, H., Ono, T., Yasuda, Y., Tokita, Y., Matsui, F., Taniguchi, M., Sonta, S., and Oohira, A. (2000). Genomic organization and expression pattern of mouse neuroglycan C in the cerebellar development. *J. Biol. Chem.* 275, 337–342.
- Aono, S., Tokita, Y., Shuo, T., Yamauchi, S., Matsui, F., Nakanishi,

- K., Hirano, K., Sano, M., and Oohira, A. (2004). Glycosylation site for chondroitin sulfate on the neural part-time proteoglycan, neuroglycan C. *J. Biol. Chem.* 279, 46536–46541.
- Berardi, N., Pizzorusso, T., Ratto, G.M., and Maffei, L. (2003). Molecular basis of plasticity in the visual cortex. *Trends Neurosci.* 26, 369–378.
- Bolshakov, V.Y., and Siegelbaum, S.A. (1995). Regulation of hippocampal transmitter release during development and long-term potentiation. *Science* 269, 1730–1734.
- Bredt, D.S., and Nicoll, R.A. (2003). AMPA receptor trafficking at excitatory synapses. *Neuron* 40, 361–379.
- Burrone, J., O'Byrne, M., and Murthy, V.N. (2002). Multiple forms of synaptic plasticity triggered by selective suppression of activity in individual neurons. *Nature* 420, 414–418.
- Cantalalops, I., Haas, K., and Cline, H.T. (2000). Postsynaptic CPG15 promotes synaptic maturation and presynaptic axon arbor elaboration in vivo. *Nat. Neurosci.* 3, 1004–1011.
- Corriveau, R.A., Huh, G.S., and Shatz, C.J. (1998). Regulation of class I MHC gene expression in the developing and mature CNS by neural activity. *Neuron* 21, 505–520.
- Du, J., Feng, L., Zaitsev, E., Je, H.S., Liu, X.W., and Lu, B. (2003). Regulation of TrkB receptor tyrosine kinase and its internalization by neuronal activity and Ca²⁺ influx. *J. Cell Biol.* 163, 385–395.
- Dumoulin, A., Rostaing, P., Bedet, C., Levi, S., Isambert, M.F., Henry, J.P., Triller, A., and Gasnier, B. (1999). Presence of the vesicular inhibitory amino acid transporter in GABAergic and glycinergic synaptic terminal boutons. *J. Cell Sci.* 112, 811–823.
- Feller, M.B. (1999). Spontaneous correlated activity in developing neural circuits. *Neuron* 22, 653–656.
- Fernandez-Chacon, R., Konigstorfer, A., Gerber, S.H., Garcia, J., Matos, M.F., Stevens, C.F., Brose, N., Rizo, J., Rosenmund, C., and Südhof, T.C. (2001). Synaptotagmin I functions as a calcium regulator of release probability. *Nature* 410, 41–49.
- Geppert, M., Bolshakov, V.Y., Siegelbaum, S.A., Takei, K., De Camilli, P., Hammer, R.E., and Südhof, T.C. (1994). The role of Rab3A in neurotransmitter release. *Nature* 369, 493–497.
- Goda, Y., and Davis, G.W. (2003). Mechanisms of synapse assembly and disassembly. *Neuron* 40, 243–264.
- Goodman, C.S., and Shatz, C.J. (1993). Developmental mechanisms that generate precise patterns of neuronal connectivity. *Cell* 72, 77–98.
- Grantyn, R., Jüttner, R., and Meier, J. (2004). Development and use-dependent modification of synaptic connections in the visual layers of the rodent superior colliculus. In *The Superior Colliculus*, W.C. Hall and A. Moschovakis, eds. (Boca Raton, FL: CRC Press), pp. 173–210.
- Han, B., and Fischbach, G.D. (1999). The release of acetylcholine receptor inducing activity (ARIA) from its transmembrane precursor in transfected fibroblasts. *J. Biol. Chem.* 274, 26407–26415.
- Hensch, T.K. (2004). Critical period regulation. *Annu. Rev. Neurosci.* 27, 549–579.
- Herzog, E., Bellenchi, G.C., Gras, C., Bernard, V., Ravassard, P., Bedet, C., Gasnier, B., Giros, B., and El Mestikawy, S. (2001). The existence of a second vesicular glutamate transporter specifies subpopulations of glutamatergic neurons. *J. Neurosci.* 21, RC181.
- Hong, S.J., Li, H., Becker, K.G., Dawson, V.L., and Dawson, T.M. (2004). Identification and analysis of plasticity-induced late-response genes. *Proc. Natl. Acad. Sci. USA* 101, 2145–2150.
- Huh, G.S., Boulanger, L.M., Du, H., Riquelme, P.A., Brotz, T.M., and Shatz, C.J. (2000). Functional requirement for class I MHC in CNS development and plasticity. *Science* 290, 2155–2159.
- Hüttner, W.B., Schiebler, W., Greengard, P., and De Camilli, P. (1983). Synapsin I (protein I), a nerve terminal-specific phosphoprotein. III. Its association with synaptic vesicles studied in a highly purified synaptic vesicle preparation. *J. Cell Biol.* 96, 1374–1388.
- Ishizaki, H., Miyoshi, J., Kamiya, H., Togawa, A., Tanaka, M., Sasaki, T., Endo, K., Mizoguchi, A., Ozawa, S., and Takai, Y. (2000). Role of rab GDP dissociation inhibitor alpha in regulating plasticity of hippocampal neurotransmission. *Proc. Natl. Acad. Sci. USA* 97, 11587–11592.
- Jessell, T.M., and Sanes, J.R. (2000). Development. The decade of the developing brain. *Curr. Opin. Neurobiol.* 10, 599–611.
- Jüttner, R., Meier, J., and Grantyn, R. (2001). Slow IPSC kinetics, low levels of alpha1 subunit expression and paired-pulse depression are distinct properties of neonatal inhibitory GABAergic synaptic connections in the mouse superior colliculus. *Eur. J. Neurosci.* 13, 2088–2098.
- Katz, L.C., and Crowley, J.C. (2002). Development of cortical circuits: lessons from ocular dominance columns. *Nat. Rev. Neurosci.* 3, 34–42.
- Kauselmann, G., Weiler, M., Wulff, P., Jessberger, S., Konietzko, U., Scafidi, J., Staubli, U., Bereiter-Hahn, J., Strebhardt, K., and Kuhl, D. (1999). The polo-like protein kinases Fnk and Snk associate with a Ca²⁺- and integrin-binding protein and are regulated dynamically with synaptic plasticity. *EMBO J.* 18, 5528–5539.
- Kim, C.H., Chung, H.J., Lee, H.K., and Huganir, R.L. (2001). Interaction of the AMPA receptor subunit GluR2/3 with PDZ domains regulates hippocampal long-term depression. *Proc. Natl. Acad. Sci. USA* 98, 11725–11730.
- Kinugasa, Y., Ishiguro, H., Tokita, Y., Oohira, A., Ohmoto, H., and Higashiyama, S. (2004). Neuroglycan C, a novel member of the neuropilin family. *Biochem. Biophys. Res. Commun.* 321, 1045–1049.
- Kirischuk, S., Jüttner, R., and Grantyn, R. (2005). Time-matched pre- and postsynaptic changes of GABAergic synaptic transmission in the developing mouse superior colliculus. *J. Physiol.* 563, 795–807.
- Kirov, S.A., Sorra, K.E., and Harris, K.M. (1999). Slices have more synapses than perfusion-fixed hippocampus from both young and mature rats. *J. Neurosci.* 19, 2876–2886.
- Konietzko, U., Kauselmann, G., Scafidi, J., Staubli, U., Mikkers, H., Berns, A., Schweizer, M., Waltereit, R., and Kuhl, D. (1999). Pim kinase expression is induced by LTP stimulation and required for the consolidation of enduring LTP. *EMBO J.* 18, 3359–3369.
- Lin, J.W., Ju, W., Foster, K., Lee, S.H., Ahmadian, G., Wyszynski, M., Wang, Y.T., and Sheng, M. (2000). Distinct molecular mechanisms and divergent endocytotic pathways of AMPA receptor internalization. *Nat. Neurosci.* 3, 1282–1290.
- McCormick, D.A. (1999). Spontaneous activity: signal or noise? *Science* 285, 541–543.
- Meier, J., and Grantyn, R. (2004). Preferential accumulation of GABAA receptor gamma2L, not gamma2S, cytoplasmic loops at rat spinal cord inhibitory synapses. *J. Physiol.* 559, 355–365.
- Meier, J., Akyeli, J., Kirischuk, S., and Grantyn, R. (2003). GABA(A) receptor activity and PKC control inhibitory synaptogenesis in CNS tissue slices. *Mol. Cell. Neurosci.* 23, 600–613.
- Mozhayeva, M.G., Sara, Y., Liu, X., and Kavalali, E.T. (2002). Development of vesicle pools during maturation of hippocampal synapses. *J. Neurosci.* 22, 654–665.
- Nedivi, E. (1999). Molecular analysis of developmental plasticity in neocortex. *J. Neurobiol.* 41, 135–147.
- Nedivi, E., Hevroni, D., Naot, D., Israeli, D., and Citri, Y. (1993). Numerous candidate plasticity-related genes revealed by differential cDNA cloning. *Nature* 363, 718–722.
- Nedivi, E., Wu, G.Y., and Cline, H.T. (1998). Promotion of dendritic growth by CPG15, an activity-induced signaling molecule. *Science* 281, 1863–1866.
- Neuhoff, V., Arold, N., Taube, D., and Ehrhardt, W. (1988). Improved staining of proteins in polyacrylamide gels including isoelectric focusing gels with clear background at nanogram sensitivity using Coomassie Brilliant Blue G-250 and R-250. *Electrophoresis* 9, 255–262.
- O'Brien, R.J., Xu, D., Petralia, R.S., Steward, O., Huganir, R.L., and Worley, P. (1999). Synaptic clustering of AMPA receptors by the extracellular immediate-early gene product Narp. *Neuron* 23, 309–323.
- O'Brien, R., Xu, D., Mi, R., Tang, X., Hopf, C., and Worley, P. (2002). Synaptically targeted narp plays an essential role in the aggrega-

- tion of AMPA receptors at excitatory synapses in cultured spinal neurons. *J. Neurosci.* 22, 4487–4498.
- Pak, D.T., and Sheng, M. (2003). Targeted protein degradation and synapse remodeling by an inducible protein kinase. *Science* 302, 1368–1373.
- Pizzorusso, T., Medini, P., Berardi, N., Chierzi, S., Fawcett, J.W., and Maffei, L. (2002). Reactivation of ocular dominance plasticity in the adult visual cortex. *Science* 298, 1248–1251.
- Poo, M.M. (2001). Neurotrophins as synaptic modulators. *Nat. Rev. Neurosci.* 2, 24–32.
- Rathjen, F.G., Wolff, J.M., Frank, R., Bonhoeffer, F., and Rutishauser, U. (1987). Membrane glycoproteins involved in neurite fasciculation. *J. Cell Biol.* 104, 343–353.
- Rosahl, T.W., Spillane, D., Missler, M., Herz, J., Selig, D.K., Wolff, J.R., Hammer, R.E., Malenka, R.C., and Sudhof, T.C. (1995). Essential functions of synapsins I and II in synaptic vesicle regulation. *Nature* 375, 488–493.
- Schoch, S., Castillo, P.E., Jo, T., Mukherjee, K., Geppert, M., Wang, Y., Schmitz, F., Malenka, R.C., and Sudhof, T.C. (2002). RIM1 α forms a protein scaffold for regulating neurotransmitter release at the active zone. *Nature* 415, 321–326.
- Schumacher, S., and Stube, E.M. (2003). Regulated binding of the fibrinogen-like domains of tenascin-R and tenascin-C to the neural EGF family member CALEB. *J. Neurochem.* 87, 1213–1223.
- Schumacher, S., Volkmer, H., Buck, F., Otto, A., Tarnok, A., Roth, S., and Rathjen, F.G. (1997). Chicken acidic leucine-rich EGF-like domain containing brain protein (CALEB), a neural member of the EGF family of differentiation factors, is implicated in neurite formation. *J. Cell Biol.* 136, 895–906.
- Schumacher, S., Jung, M., Norenberg, U., Dorner, A., Chiquet-Ehrismann, R., Stuermer, C.A., and Rathjen, F.G. (2001). CALEB binds via its acidic stretch to the fibrinogen-like domain of tenascin-C or tenascin-R and its expression is dynamically regulated after optic nerve lesion. *J. Biol. Chem.* 276, 7337–7345.
- Steen, H., and Mann, M. (2004). The ABC's (and XYZ's) of peptide sequencing. *Nat. Rev. Mol. Cell Biol.* 5, 699–711.
- Tsui, C.C., Copeland, N.G., Gilbert, D.J., Jenkins, N.A., Barnes, C., and Worley, P.F. (1996). Narp, a novel member of the pentraxin family, promotes neurite outgrowth and is dynamically regulated by neuronal activity. *J. Neurosci.* 16, 2463–2478.
- Urban, S., Lee, J.R., and Freeman, M. (2002). A family of Rhomboid intramembrane proteases activates all *Drosophila* membrane-tethered EGF ligands. *EMBO J.* 21, 4277–4286.
- Verhage, M., Maia, A.S., Plomp, J.J., Brussaard, A.B., Heeroma, J.H., Vermeer, H., Toonen, R.F., Hammer, R.E., van den Berg, T.K., Missler, M., et al. (2000). Synaptic assembly of the brain in the absence of neurotransmitter secretion. *Science* 287, 864–869.
- West, A.E., Chen, W.G., Dalva, M.B., Dolmetsch, R.E., Kornhauser, J.M., Shaywitz, A.J., Takasu, M.A., Tao, X., and Greenberg, M.E. (2001). Calcium regulation of neuronal gene expression. *Proc. Natl. Acad. Sci. USA* 98, 11024–11031.
- Yasuda, Y., Tokita, Y., Aono, S., Matsui, F., Ono, T., Sonta, S., Watanabe, E., Nakanishi, Y., and Oohira, A. (1998). Cloning and chromosomal mapping of the human gene of neuroglycan C (NGC), a neural transmembrane chondroitin sulfate proteoglycan with an EGF module. *Neurosci. Res.* 32, 313–322.